Calculation of the Energetics for the Oligomerization of Gas Phase HgO and HgS and for the Solvolysis of Crystalline HgO and HgS

J. A. Tossell*

Department of Chemistry and Biochemistry, University of Maryland, College Park, Maryland 20742

Received: October 31, 2005; In Final Form: December 21, 2005

Recent experimental studies indicate that gaseous elemental Hg (GEM) is rapidly oxidized to Hg(II) compounds, known collectively as reactive gaseous Hg (RGM), in Arctic and Antarctic regions after polar sunrise. The reduction in GEM is correlated with a reduction in surface O_3 concentration, which is thought to be caused by photochemically initiated catalytic reactions involving halogen species, particularly Br and BrO. Initially, the reaction of Hg^0 and BrO to produce HgO and Br was thought to be the dominant reaction, but recent theoretical studies have decisively shown that this reaction is highly endoergic due to the low stability of monomeric gas-phase HgO. This result is in conflict with experimental data on the energetics of the species existing in the vapor over heated HgO (s). One possible explanation for this discrepancy is the existence of highly stable oligomers formed from HgO. Recent high-level quantum calculations on the dimers of HgO and HgS support this concept. In the present work, we systematically examine the structures, stabilities, and other properties of closed $(HgX)_n$ ring-type oligomers, $n = 2$, 3, 4, and 6, X = O, S, as well as infinite one-dimensional (1D) polymers of HgX (studied by using the periodic boundary condition DFT implementation in GAUSSIAN03). We find that the HgX ring oligomers become systematically more stable (per HgX unit) as n increases but that this stability levels off around $n = 4-6$. We also find that the 1D chain polymers are only marginally more stable than the $n = 6$ oligomers. To estimate the energies of interaction between the chains in the 3-dimensional (3D) crystal structures of HgX (s), we adopt a cluster model and use the MP2 method to describe the interchain dispersion interactions. We have also obtained optimized geometries for open chain triplets for the dimers, finding them to be substantially more stable than the closed ringlike dimeric species previously described. Trends in relative energies and structures indicate that the higher n oligomers are fairly normal Hg(II) compounds that can be accurately described at low computational levels, as opposed to the monomer and dimer, which possess highly unusual bonding properties and require high-level methods for their description. Nonetheless, even the high n ring, oligomers show close approach of Hg atoms, consistent with a metallophilic-type stabilization. Calculated free energies for the interaction of HgO with H_2O and with simple models for silicate surfaces are highly favorable, indicating that hydration and surface effects will greatly promote the formation of such species. Molecular cluster models of the HgX surface such as $Hg_2X(XH)_2$ are used to calculate the energetics for solvolysis reactions with H_2O or H_2S, obtaining good agreement with experiment for the energetics of the dissolution reaction of HgS (s, cinnabar) with H_2S.

Introduction

Hg is an environmental pollutant that is found in the atmosphere, natural waters, and the human body. In the atmosphere, elemental Hg and small molecule halides and oxides are thought to be most important species, while in aqueous solution, sulfidic species, obtained from the dissolution of solid sulfides, are often important. Within the body, organometallic Hg compounds and species with Hg−S bonds are most important. Thus, environmentally important reactions of Hg involve both Hg oxides and sulfides and small molecules, larger oligomeric species, and bulk solids.

Gas-phase elemental Hg (GEM) has both natural and anthropogenic sources. In the atmosphere, elemental gas-phase Hg^0 undergoes long-range atmospheric transport. Several recent studies indicate that GEM is rapidly oxidized to Hg(II) compounds, known as reactive gaseous mercury (RGM) in Arctic regions after polar sunrise.[1−4] The reduction in GEM is correlated with a reduction in surface O_3 concentration, which is thought to be caused by photochemically initiated catalytic reactions involving halogen species, particularly Br and BrO[2]. The oxidizing agents for GEM are also thought to be predominantly halogen atoms or halogen oxide free radicals. Modeling of the kinetics and energetics of the process[5−8] has been carried out previously by using tabulated experimental heat of formation data on assumed reactants and products. Experimental studies have determined the rate of loss of Hg^0 in the presence of various oxidants, but in some cases, the products were not clearly identified.[9−11] Ariya et al.[11] have noted that experimental data on the gaseous reactions of Hg^0 is very limited, compared to the extensive data on the solution chemistry of Hg. This is due to the small concentrations of Hg^0 species under atmospheric conditions, the low volatility of products, and the strong effects of water vapor and surfaces on the reaction energetics and kinetics.

There is only limited experimental information on the structure and stability of apparent gas-phase or matrix-isolated HgO.[12] There have also been only a relatively small number of calculations on the properties of Hg compounds within the

* Corresponding author. E-mail: tossell@chem.umd.edu.

10.1021/jp056280s CCC: $33.50
Published on Web 01/27/2006

theoretical inorganic literature.[13,14] However, in several recent theoretical studies,[15−17] gas-phase diatomic HgO was studied at high computational levels and was found to be barely stable with respect to Hg^0 and ground-state O, in apparent contradiction to the experimental data.[18] The discrepancy between calculated and (apparent) experimental heats of formation is around 50 kcal/mol! It has been suggested that the species actually characterized experimentally was a triplet state of the HgO dimer, which was calculated to be much more stable than the monomer,[17] but other more complicated HgO-derived species were not considered. The structures and properties of some species in aqueous solution derived from HgS have also been studied by using theoretical methods,[18] but not species derived from HgO.

To determine Hg speciation, it is desirable to characterize the energetics for some of the possible gas-phase and aqueous solution oxidation reactions of Hg^0 and for the oligomerization reactions of HgO and HgS by using modern quantum mechanical techniques.

Computational Methods

Standard methods of molecular quantum mechanics have been used, primarily the Hartree−Fock (HF) method, the Moller−Plessett many-body perturbation theory method to second order (MP2), and the coupled cluster with single and double substitutions (CCSD), along with various density functional methods. All the methods used are described in standard computational chemistry monographs[19] The MP2 and CCSD methods incorporate correlation in the motion of electrons,[20−22] which is neglected at the HF level. They typically provide much more accurate bond energies and somewhat better equilibrium geometries than does the HF method. However, they are more demanding of computer time than HF, particularly the CCSD method, and scale with high powers of the number of orbitals. The basis sets used to expand the molecular orbitals were of double-ζ valence-electron only, relativistic effective core potential type,[23] which we designate SBK, with added polarization functions on all the atoms. For Hg, single *f* polarization functions with an exponent of 0.486 (from ref 14) are employed. For all the species considered, we have determined equilibrium geometries in the gas-phase and have evaluated vibrational frequencies, zero-point vibrational energies (ZPE) and vibrational, rotational, and translational (VRT) contributions to the gas-phase free energy at 25 °C. The necessary equations for the ZPE and VRT contributions are incorporated into the quantum chemical software.

To approximate hydration energies, we have used the COSMO (conductor-like screening MO method[24]) version of the self-consistent reaction field polarizable continuum method. This is a very rapid and efficient technique that utilizes a nonspherical cavity about the solute and gives results very similar to those from older nonspherical cavity polarizable continuum models, but at much less computational cost. Nonetheless, it still suffers from the main ambiguity of polarizable continuum models, the lack of uniqueness in the choice of the solute cavity. It is important to realize that any polarizable continuum model of hydration involves very serious approximations and that the hydration energy differences evaluated for reactions, particularly those involving ions, are invariably much less accurate than are the corresponding gas-phase energies. We used the quantum chemical software GAMESS[25] and GAUSSIAN98[26a] and GAUSSIAN03[26b] for the calculations. Figures of the molecules studied were created with GaussView.[27]

TABLE 1: Calculated Relative Energies (in kcal/mol) of a HgO Unit in a $(HgO)_n$ Ring, Compared to that of Monomeric Singlet HgO (g) Using BLYP, PBE, MP2, and CCSD Methods, with Polarized Relativistic Effective Core Potential Basis Sets

molecular unit/method	Hg_2O_2 (g) O−Hg_2−O isomer	Hg_3O_3 (g)	Hg_4O_4 (g)	Hg_6O_6 (g)	HgO (1D crystal)
BLYP	−19.2	−46.7	−59.1	−63.3	−63.9
PBE	−23.1	−53.3	−66.1	−70.2	−70.5
MP2	−21.8	−58.0	−72.6	−76.6	n.a.
CCSD	−18.1	−52.7	n.a.[a]	n.a.[a]	n.a.[a]

[a] n.a. = not attempted.

TABLE 2: Calculated Relative Energies (in kcal/mol) of a HgS Unit in a $(HgS)_n$ Ring, Compared to that of Monomeric Singlet HgS (g), Using BLYP, PBE, MP2, and CCSD Methods, with Polarized Relativistic Effective Core Potential Basis Sets

molecular unit/method	Hg_2S_2(g) S−Hg_2−S isomer	Hg_3S_3(g)	Hg_4S_4(g)	Hg_6S_6(g)	HgS (1D crystal)
BLYP	−24.9	−48.3	−54.2	−55.0	−55.2
PBE	−30.1	−56.0	−61.9	−62.9	−62.5
MP2	−33.2	−62.2	−69.5	−70.3	n.a.
CCSD	−28.0	−58.4	n.a.[a]	n.a.[a]	n.a.[a]

[a] n. a. = not attempted.

TABLE 3: Calculated Energies Relative to that of the X···Hg_2···X Singlet Dimer 1 (in kcal/mol) for Ring and Chain Dimers of HgO and HgS, Obtained at Various Computational Levels

molecule	ΔE (BLYP)	ΔE (MP2)	ΔE (CCSD)	ΔE (CCSD(T)) @CCSD
Hg_2O_2, ring singlet 1	0	0	0	0
ring singlet 2	n.c.[a]	+0.3	+4.0	+5.4
ring triplet 1	−5.5	+16.7	−4.7	+2.6
ring triplet 2	n.c.[a]	−7.0	−22.2	−10.3
chain triplet	−34.6	−24.4	−45.2	−29.4
Hg_2S_2, ring singlet 1	0	0	0	n.a.[b]
ring singlet 2	n.c.[a]	−10.1	+21.2	n.a.[b]
ring triplet 1	+16.7	+14.2	+17.3	n.a.[b]
chain triplet	−9.1	−9.0	−13.2	n.a.[b]

[a] n.c. = SCF not converged. [b] n.a. = not attempted.

Results and Discussion

Structures and Energies of HgX Oligomers. Energies at optimized geometries obtained by a number of different methods (BLYP,[28a,b] PBE,[28c] MP2, and CCSD) are given for the oligomers of HgO and HgS in Tables 1−3. We observed the increase in stability from the monomer and the dimer seen in previous calculations.[17] Our calculated energy per HgO unit changes by −18.1 kcal/mol between the singlet state of the monomer and the singlet state of the O−Hg_2−O isomer of the dimer (ring singlet 1) at the CCSD level, while the corresponding difference at the highest level used by Filatov and Cremer (Feenberg-scaled MP4 with a larger basis set) in ref 17 was −25.1 kcal.mol. We also found two different singlet and triplet isomers, one with a short Hg−Hg bond and one with a short X−X bond. We refer to these as ring isomers of type 1 and 2 and show them in Figure 1.

We have also systematically explored the structure and stability of ring oligomers for $n = 3$, 4, and 6 and chain isomers for $n = 2$. For the BLYP, PBE, MP2, and CCSD methods, the progressive stabilization of $(HgO)_n$ is consistent, and uniform pictures of the geometries of some of these species are also shown in Figure 1. Bond lines are drawn in these figures by using an internuclear distance criterion, so they should be

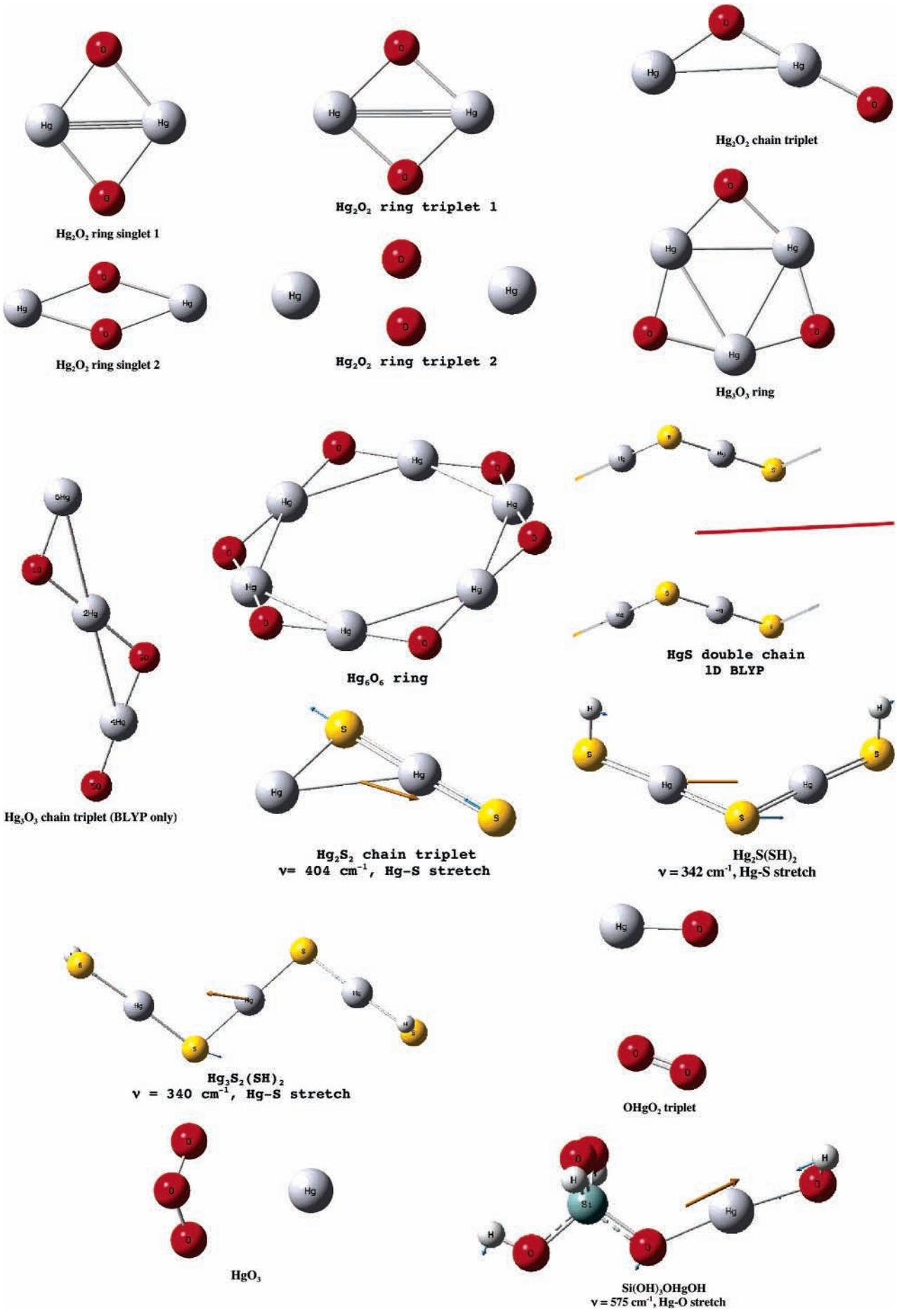

Figure 1. Geometries calculated at the MP2 level ("bonds" drawn using a distance criterion).

TABLE 4: Calculated Geometries and Relative Energies (in kcal/mol vs Ring Singlet 1) for Four Different Isomers of Hg_2O_2, from Results of Ref 17 (Geometries at IORAmm/B3LYP and Energies at $FE^{(4)}_{\lambda(3)}$) and Present (CCSD Geometries and CCSD(T) Energies)

	ref 17			present		
	R(Hg−Hg)	R(O−O)	ΔE	R(Hg−Hg)	R(O−O)	ΔE
ring singlet 1	2.77	3.26	0	2.78	3.31	0
ring singlet 2	4.19	1.62	+10.2	4.18	1.66	+5.4
ring triplet 1	3.02	3.06	−66.3	3.09	3.09	+2.6
ring triplet 2	4.82	1.37	−69.5	4.81	1.41	−10.3
chain triplet	not found			3.37	3.91	−29.4

considered mostly guides to the eye. However, compared to more ordinary ring oligomers of other metallic oxides, these compounds appear to be distorted so as to give short metal−metal distances. For example, in the ring isomer of Hg_3O_3 (see Figure 1) evaluated at the CCSD level, the calculated Hg−Hg distance is only 2.90 Å, only slightly longer than the calculated Hg−Hg distance of 2.78 Å in the singlet O−Hg_2−O isomer of Hg_2O_2. Thus, the Hg−Hg bonding found in singlet 1 of the dimer is still retained, to a large extent in the higher oligomers. There is a smooth decrease in the energy per HgX unit as n increases, until the trend flattens out between $n = 4$ and 6. The energies per HgX unit for one-dimensional (1D) chains (obtained used the periodic boundary condition approach implemented in GAUSSIAN03) are only very slightly lower than those for the $n = 6$ oligomer. This is true for both HgO and HgS species. Unfortunately, we have 1D periodic chain results for only the pure DFT functionals, BLYP and PBE, because computational costs proved too high when nonlocal HF or hybrid potentials were used.

For the dimers of HgO and HgS, we have examined the relative stabilities of the different isomers at a number of levels of theory, as shown in Table 3. It is clear that while the stabilities of the singlets do not vary enormously with the level of treatment, the triplet states show large changes, even from CCSD to CCSD(T). It is not our main purpose in this paper to systematically compare our structures and energies for the dimeric species with those previously determined.[17] We are more interested in the larger ring-type oligomers and in possible chain oligomers. In general, our optimized *structures* obtained by using polarized double-ζ effective potential basis sets at the CCSD level and those of Filatov and Cremer, obtained by using considerably larger basis sets at the B3LYP level, are in quite good agreement, with Hg−Hg and O−O distances differing by at most 0.1 Å between the two approaches. These results are shown in Table 4. Our relative energies for the two different singlet states of Hg_2O_2 and for that energy compared to singlet HgO are also in reasonably good agreement. We do differ substantially in the relative energies (with respect to singlet 1 of Hg_2O_2) for the triplet energies, even with our very similar geometries, as also shown in Table 4. The Feenberg-extrapolated MP4 relative energies of the triplets are considerably lower than our relative CCSD(T) energies, with differences as large as 50 kcal/mol Hg_2O_2. As noted in ref 15, even for monomeric HgO, the triplet state is difficult to describe because it is close to the point at which an ionic charge distribution is expected to change to a covalent one, and so single reference methods may give poor results. It is also, of course, true that the full accuracy of the CCSD method may not be obtained by using our small basis sets. Therefore, although the triplet states of Hg_2O_2 are reliably characterized in terms of structure, there is some doubt about their relative energies.

Note that we have also not considered spin−orbit coupling effects because it would be extremely difficult to do so for the polyatomic species we are considering. Shepler and Peterson (ref 15) did calculate spin−orbit effects by using a multireference CI approach for HgO and found that the ground electronic state was stabilized by 2.4 kcal/mol. In this case, the singlet σ and triplet π states were almost degenerate in the absence of spin−orbit coupling. Certainly, a further analysis of spin−orbit effects would be desirable for the singlet and triplet states of the oligomers, but if the effects are no larger than in monomeric HgO, the overall stability of the states would be unchanged.

TABLE 5: Calculated VRT Contributions to Gas-Phase Free Energies at 25 °C (in kcal/mol) Per HgX Unit, Relative to Singlet Monomer, Using BLYP

	$(HgX)_n$ ring singlet 1	$(HgX)_n$ chain triplet
Hg_2O_2	+5.0	+4.0
Hg_3O_3	+7.8	+6.8
Hg_4O_4	+9.0	n.c.
Hg_2S_2	+5.1	+3.7
Hg_3S_3	+7.5	n.c.
Hg_4S_4	+8.2	n.c.

[a] n.c. = SCF not converged.

TABLE 6: Calculated Geometries for Ring Form of Hg_3O_3, Using Various Methods

method	R(Hg−O)	R(Hg−Hg)	∠O−Hg−O	∠Hg−O−Hg
HF	2.047	3.020	144.9	95.1
BLYP	2.127	2.988	150.5	89.3
PBE	2.097	2.919	151.7	88.2
MP2	2.067	2.838	153.3	86.7
CCSD	2.063	2.900	150.5	89.3

To assess the thermodynamic stability of the different oligomeric species, we also need to consider zero-point vibrational energy and finite T contributions to the enthalpy and the entropy. In Table 5, we present the total vibrational, rotational, and translational contributions to the gas-phase free energies at 25 °C per HgX unit for the HgX species, $n = 2$, 3, and 4, obtained at the BLYP level. It is clear that the ΔG_{VRT} contributions become somewhat more positive as n increases due to the entropic penalty associated with reducing the number of molecules per HgX unit. This opposes the trend of increasing stability with increasing n, but the entropic effect is not large enough to reverse the trend for $n = 2-4$. Unfortunately, the geometry optimization proved so time-consuming for the Hg_6S_6 species that we have not determined vibrational frequencies for it and so cannot assess ΔG_{VRT}. We also find a slight difference in this quantity for the ring singlet and chain triplets, but not enough to change the overall order of stability.

We find the triplet state of the ringlike Hg−O_2−Hg isomer to be overall the most stable form of the closed ringlike dimers, lying 27.8 kcal/mol HgO below the singlet monomer at the CCSD(T) level. For this particular species, we also calculated a MP4(SDTQ) result that gave a lowering of 22.8 kcal/mol, compared to the singlet state of the monomer at the same level. Of course, for the calculations on monomers and dimers in ref 17, much larger basis sets were employed than in our study. Thus, our results for the HgO ring dimers agree with ref 17 qualitatively, but there is a substantial quantitative discrepancy.

Moreover, we have also found *open-chain* triplet states for both the HgO and HgS dimers, which we calculate to be more stable than any of the singlet or triplet ring isomers. These open chain species, whose relative energies are given in Table 3 and whose geometries are given for the HgS case in Table 7, look very much like fragments from the 1D periodic chain. In fact, the starting geometries for their energy optimizations were taken from the crystal structures of HgO and HgS. We have confirmed that both the Hg_2O_2 and Hg_2S_2 chain triplets have all positive

TABLE 7: Calculated Geometries for HgS Oligomers, Using the MP2 Method

species	R(Hg−S)	R(Hg−Hg)
Hg_2S_2, chain triplet	2.30, 2.48	3.37
Hg_2S_2, ring singlet	2.45	2.72
Hg_3S_3, ring singlet	2.35	3.00
Hg_4S_4, ring singlet	2.32	3.26
Hg_6S_6, ring singlet	2.31	3.32

vibrational frequencies at both the BLYP and MP2 levels. Plots of a Hg−O stretching mode at 660 cm^{-1} for chain triplet Hg_2O_2 and a stretching mode of chain triplet Hg_2S_2 at 404 cm^{-1} (both obtained at the MP2 level) are shown in Figure 1. We attempted to characterize similar chain triplets for the HgX trimers, but were able to get SCF convergence at only the BLYP level and only for the oxide, Hg_3O_3. The structure of this chain triplet is also shown in Figure 1 and looks like a fragment from the infinite 1D chain of HgO (s). It is not clear whether the difficulty in finding chain isomers for the larger oligomers reflects a fundamental instability of such species or simply poor choices of the starting geometry. Indeed, even for the HgX chain triplet dimers, only some of the starting geometries we tried led to SCF convergence.

Calculated bond distances are given for a representative molecule Hg_3O_3 in Table 6, obtained with a number of different methods. Changing the quantum mechanical method for this molecule produces only a modest change in geometric parameters. In general, we find that both structural and energetic parameters show less change with method for the larger oligomers than for Hg. Therefore, we do not need to use such accurate and demanding methods as were required to get converged results for the monomer and dimer. This is certainly an encouraging result because applying CCSD methods and extrapolating to the basis set limit for Hg_6S_6 would be a daunting task.

Calculated geometries for the $n = 2$ and 3 oligomers of HgS obtained by using the MP2 method are given in Table 7. The lowest energy Hg_2S_2 species is calculated to be the chain triplet, which has two inequivalent Hg−S distances of 2.30 and 2.48 Å. Studies of the HgS species in sulfidic solutions[29a] by using XAS have identified a two-coordinate Hg species with an experimental Hg−S bond distance of 2.30 Å, while studies of HgS precipitates[29b] formed at lower pH and then aged showed initially two-coordinate species with Hg−S distances of 2.35 and 2.97 Å. MP2 calculations on $Hg_2S(SH)_2$, which can be formed by reacting Hg_2S_2 with H_2S, also shows Hg−S distances of 2.30 Å. It may be that the larger of the Hg−S distances observed in the precipitate arises from the approach of chainlike units, although the S in the second neighbor position to Hg in crystalline cinnabar is at a much larger distance, around 4.15 Å.

Structures and Energies of HgX Solids. At the BLYP level, we obtained optimized Hg−X distances of 2.022 and 2.411 Å for 1D periodic chain structures of HgO and HgS, respectively, while the bond distances in the real three-dimensional (3D) (but quasi-1D chain) structures are[30,31] 2.04 and 2.36 Å, respectively. A 1D BLYP calculation on a HgS double chain unit gives the same Hg−S distance to within 0.01 Å. However, the optimized interchain distances are much too large in this BLYP calculation; the calculated Hg−Hg distance is 7.07 Å, while the experimental distance is 4.15 Å. Thus, the BLYP calculation completely misses the stabilizing interaction of the two HgS chains, a relativity-enhanced correlation effect. This problem with pure DFT potentials has been previously noted.[32] Calculations using the CASTEP DFT program and the BP86 potential seem to overcome this problem to a considerable extent, giving interchain distances that are only moderately exaggerated.[33] We have attempted to correct for this by calculating the interaction energy at the MP2 level of two different discrete fragments from this chain, $Hg_2S(SH)_2$ and $Hg_3S_2(SH)_2$, which we will be using again to estimate the energies of hydrolysis-type reactions. MP2 calculations performed for pairs of such molecules give an energy minimum at interchain separations around 4.1−4.2 Å, consistent with the experimental structure. We calculate the MP2 interaction energies as a function of interchain distance for each fragment molecule and then take the difference of these fragment energies to determine a MP2 stabilization energy for a fragment HgS unit. For HgS, this gives an interchain stabilization energy of about 3.6 kcal/mol. Because each chain has four neighboring chains, the total stabilization is about 14.4 kcal/mol HgS. Ruiz and Payne have used a slightly different procedure from their CASTEP BP86 calculations[33] to evaluate interchain stabilization energies of 5.6 kcal/mol HgS.

Energetics for Reactions of HgX Oligomers and Dissolution of HgX Solids. We have also evaluated the energetics for several reactions of the HgX oligomers in both the gas phase and aqueous solution. Our goals are twofold: (1) to evaluate possible reactions of the highly unstable monomers and dimers that can lead to more stable products, and (2) to use small molecules as models for reactions in which extended solids react with solvent. For example, in the first category, we have examined a number of possible reactions of HgO and Hg_2O_2. In the second category, we have considered reactions of $Hg_2X(XH)_2$ and $Hg_3X_2(XH)_2$ as models for crystalline HgO and HgS, focusing upon their reaction with H_2O or H_2S. This allows us to simulate energetics for the dissolution reactions of crystalline Hg compounds, including the mineral cinnabar, HgS.

Experimental studies[34] on the reaction of gas-phase elemental Hg with BrO and O_3 have identified HgO products obtained from the walls of the reaction vessel by using mass spectrometry. Because the gas-phase reactions of Hg with BrO or O_3 to give HgO have strongly positive free energies, there must be either surface or solvent effects favoring the formation of a HgO-type product. It has been suggested[35] that HgO_3 is an intermediate in this process, and we indeed find that there is a stable van der Waals-type complex of Hg and O_3, just as previous computational studies[36] have found such a complex for PbO_3. It has been suggested that HgO_3 may isomerizes to a species such as $OHgO_2$, which can then react favorably with surfaces to produce HgO. In the Pb, O_3 system, there is indeed a $OPbO_2$ isomer that is more stable than PbO_3. However, for the Hg, O_3 case, the $OHgO_2$ isomer lies high in energy above HgO_3 due to the weakness of the Hg−O bond.

A full evaluation of the interaction of HgO or related species with models for surfaces is outside the boundaries of this work, but we have considered the simplest type of interaction expected to occur with silica surfaces. These energies are presented in Table 8. We have calculated the energy for insertion of HgO or HgO_3 into a surface silanol group modeled as $Si(OH)_4$. This is clearly a very simple and approximate model for the silica surface which the Hg species would encounter in a typical vacuum experiment, but it illustrates an important point. The reaction is enormously favorable, by 50−60 kcal/mol, mainly because of the low stability of gas-phase HgO. HgO also reacts exoenergically with H_2O to give $Hg(OH)_2$, which has been identified and characterized by IR spectroscopy in inert gas matrixes.[37] This is consistent with our calculated energetics in Table 8. Any reaction which can convert one-coordinate Hg in HgO to a fully two-coordinate form of Hg will be highly

TABLE 8: Calculated Energetics (in kcal/mol) in the Gas Phase for Reactions of HgO with O_3 to Form HgO_3, $OHgO_2$, and $HgO + O_2$ and for Reactions of HgO and HgO_3 with $Si(OH)_4$ and H_2O

reaction	BLYP	MP2	CCSD
$Hg + O_3 \rightleftharpoons HgO_3$ singlet	−4.0	−4.3	−4.6
$Hg + O_3 \rightleftharpoons OHgO_2$ triplet	+16.2	+38.1	+11.5
$Hg + O_3 \rightleftharpoons HgO + O_2$ triplet	+20.4	+27.7	+12.9
$HgO + Si(OH)_4 \rightleftharpoons Si(OH)_3OHgOH$	−64.4	−77.9	n.a.
$HgO_3 + Si(OH)_4 \rightleftharpoons Si(OH)_3OHgOH + O_2$	−40.0	−45.9	n.a.
$HgO + H_2O \rightleftharpoons Hg(OH)_2$	−62.6	−68.4	−69.8

[a] n.a. = not attempted.

TABLE 9: Calculated Energetics (in kcal/mol) in the Gas Phase for Solvolysis Reactions of $Hg_2O(OH)_2$ and $Hg_2S(SH)_2$, Using Various Methods

reaction	BLYP	MP2	CCSD @MP2 geom.	CCSD
$Hg_2O(OH)_2 + H_2O \rightleftharpoons 2Hg(OH)_2$	+1.4	+7.8	+4.3	+4.7
$Hg_2S(SH)_2 + H_2S \rightleftharpoons 2Hg(SH)_2$	+2.5	+8.2	+4.8	+5.0

favored. Even the reaction of the chain triplet (lowest energy) form of Hg_2O_2 with H_2O to give $Hg_2O(OH)_2$ has a gas-phase free energy of −60.6 kcal/mol (at the CCSD level). Thus, the strong effect of surfaces and moisture on the reactions of elemental Hg are a direct result of the low stability of monomeric and dimeric HgO.

We can also examine the process of breakdown in aqueous solution for the polymeric or oligomeric species. For example, we can use our calculated energetics to determine the free energy changes for the dissolution of minerals. General observations on the solubility and reactivity of HgO and HgS are that HgO is fairly soluble in water, while HgS is only very slightly soluble in pure water but dissolves more readily in sulfidic solutions. For the reaction of cinnabar, HgS (s), with H_2S to give $Hg(SH)_2$:

$$\text{Hg (s, cinnabar)} + H_2S\,(aq) \rightleftharpoons Hg(SH)_2\,(aq) \qquad (1)$$

which we obtain by using the experimental equilibrium constants[38] and by using 6.9 for pK_{a1} of H_2S, a log equilibrium constant of −5.9, corresponding at 25 °C to a free energy change of about +8.0 kcal/mol.

The basic chemical step in this dissolution process in the breaking of a Hg−X−Hg bond within the chain to give smaller species with Hg−XH bonds. A simple reaction describing such a process for HgS would be:

$$Hg_2S(SH)_2 + H_2S \rightleftharpoons 2\,Hg(SH)_2 \qquad (2)$$

Of course, using a larger oligomer, e.g., $Hg_3S_2(SH)_2$ or a periodic 1D HgS chain, might well be a better model as long as we could evaluate all the energetic terms accurately. For the reaction shown just above, we can indeed evaluate the energy at a high quantum mechanical level, e.g., CCSD, evaluate VRT contributions to the gas-phase free energy at some reasonable level, and obtain hydration free energy contributions from a polarizable continuum model. We could also use slightly larger molecular models, perhaps describing them at a somewhat lower quantum mechanical level, to test for convergence.

Results are presented in Tables 9 and 10 for these approaches. We see that the total reaction free energy is in quite reasonable absolute agreement with experiment for the HgS + H_2S case and that trends in calculated free energies are in agreement with observed experimental trends; HgS (s) is highly insoluble in pure water but fairly soluble when H_2S is present, while HgO (s) is fairly soluble in water. If we change our model for the

TABLE 10: Calculated Contributions to Free Energy of Reaction (in kcal/mol) in Solution for Reaction of $Hg_2S(SH)_2$ with H_2S or H_2O and of $HgO(OH)_2$ with H_2O

contribution	$HgS(SH)_2$ and H_2S	$HgS(SH)_2$ and H_2O	$HgO(OH)_2$ and H_2O
energy change in gas phase (CCSD value)	+5.0	+28.6	+4.3
VRT contribution to gas-phase free energy	+0.1	−1.7	−1.4
hydration contribution to free energy (using CPCM)	+1.9	−0.6	−5.0
total reaction free energy	+7.0 expt +8.0	+26.3	−2.1

TABLE 11: Calculated Vibrational Frequencies (in cm^{-1}) and Energies (in kcal/mol) for $Hg_2S(SH)_2$ and $Hg_3S_2(SH)_2$

molecule	$Hg_2S(SH)_2$	$Hg_3S_2(SH)_2$
ZPE	11.8	12.9
ΔH_{VRT}	18.8	22.6
ΔG_{VRT}	−14.6	−19.7
υ (cm^{-1})	31, 67, 70, 82, 85, 87, 103, 282, 295, 333, 342, 671, 672, 2564, 2564	9, 21, 28, 59, 61, 73, 82, 85, 90, 93, 102, 276, 292, 299, 330, 340, 342, 670, 672, 2564, 2564

reactant from $Hg_2S(SH)_2$ to $Hg_3S_2(SH)_2$, the energy for the gas-phase dissolution reaction at the MP2 level (the highest level feasible for the larger molecule) goes from 7.8 to 8.3 kcal/mol, so we have reasonable stability with respect to cluster size.

Employing a 1D chain model for HgX is more difficult. We know that the DFT approach that we are forced to use for the PBC calculations does not give a good description of the dispersion interaction between chains. For example, for reaction 1, we calculate a gas-phase energy at the BLYP level of +1.3 kcal/mol, which seems quite similar to the gas-phase energy for the solvolysis reaction of $Hg_2S(SH)_2$, the second reaction in Table 8. However, calculating the other terms in the free energy change for the real reaction at the aqueous interface with cinnabar is very difficult. We must first add to the stability of HgS, cinnabar, the interaction energy of a single chain with the four surrounding chains, which on the basis of the DFT calculations of Ruiz and Payne could be as large as 4(−5.6) = −22.4 kcal/mol. Our MP2 calculations using fixed monomer geometries suggest a considerably smaller value of 4(−3.6) = −14.4 kcal/mol. We must then evaluate the value of ΔG_{VRT} for HgS, cinnabar, which would require at the very least the zero-point vibrational energy of the solid. The experimental vibrational frequencies[39] are 43 and 256 for the two a_1' modes, 36, 102, and 336 for the three a_2'' modes, and 83, 92, 100, 280, and 343 for the e′ modes (all in cm^{-1}), giving a ZPE of about 3.76 kcal for the trimolecular hexagonal unit cell of HgS, or about 1.25 kcal/mol per HgS unit. The difference in calculated ZPE between $Hg_2S(SH)_2$ and $Hg_3S_2(SH)_2$ (at the BLYP level) is about 1.1 kcal/mol, reasonably consistent with the experimental data above. Once we have taken out the four highest-energy calculated frequencies for these molecular models, the modes from about 670 to 2560 cm^{-1}, which correspond to bending and stretching modes of the H atoms, the correspondence of calculated and experimental frequencies is good. The modes calculated around 290−350 cm^{-1} correspond to Hg−S stretching vibrations, and those around 80−100 cm^{-1} correspond to bending modes of the −Hg−S− framework.

In Table 11, we collect vibrational and energetic data for the two molecular models used for the −Hg−S− 1D chain solids. Their difference in ΔG_{VRT} is about −5.1 kcal/mol. Using −5.1

kcal/mol as the ΔG_{VRT} value for HgS (s, cinnabar) in reaction 1 gives an overall ΔG_{VRT} contribution of −0.7 kcal/mol to the reaction energy. ΔG_{COSMO} can in principle be obtained by using only the H_2S (aq) and $Hg(SH)_2$ (aq) hydration free energies, giving a value around −14.4 kcal/mol for this contribution to the reaction free energy. Remember that the experimental value for the free energy change of the solvolyis reaction for HgS, cinnabar, is +8.0 kcal/mol. To obtain a calculated value close to this, we necessarily need the gas-phase energy to be highly positive. Thus, the molecular and crystal approaches to the solvolysis reactions are very different both qualitatively and quantitatively. In the molecular approach, we focus upon the breaking of the Hg−S−Hg bond, which is slightly unfavorable from the energetic point of view in the gas-phase (by +2.5 kcal at the B3LYP level and +5.0 kcal/mol at the CCSD level, Table 9) but becomes more favorable in aqueous solution due to hydration of the product. In the solid approach, we are considering a much more dramatic change in which energetic stabilization both within the −Hg−S− chain and between chains is lost, but this loss is compensated by the large hydration energy of the product $Hg(SH)_2$. Conceivably these models might actually correspond to different steps in the process, for which the present experimental data resolves only averaged energies and rates.

Conclusions

We have analyzed computationally changes in structure and stability of HgX species starting with two extremes: the diatomic monomer in the gas phase and the 3D (although quasi-1D) crystalline solid.

We confirm earlier calculations that identified two different closed-ring isomeric forms of the dimer for the HgO case along with two different stable spin states, but we also identify new open-chain triplet states for both HgO and HgS, which have geometries similar to fragments from the 1D chains found in the crystals. The energies of these open-chain species have been evaluated at the CCSD(T) level, and calculations at the MP2 level have confirmed that they are indeed local minima. For the higher oligomers $(HgX)_n$, we have found closed-ring singlet states that increase in stability with increasing n. For $n = 6$, the stabilities per HgX unit are very close to the stability for the 1D chain polymer. These higher oligomers retain some unusual bonding characteristics, with short Hg−Hg metallophilic interactions.

We have examined the energetics for the reactions of HgO or HgO_3 with H_2O or with a very simple $Si(OH)_4$ model for a silicate surface, establishing that such reactions are very exothermic and that HgO and HgO_3 will be unstable in the presence of moisture or surfaces. This provides a mechanism for stabilizing HgO-derived species as products of the oxidation of elemental Hg^0 by BrO. However, it may well be that the predominant process for Hg^0 oxidation may be the formation of $HgBr_2$, which is calculated[40] to be a favorable process with a rate consistent with experiment.

We have also studied solvolysis reactions that break down the HgX solids and oligomeric units derived from them to form solution species such as $Hg(OH)_2$ and $Hg(SH)_2$. For such reactions, the energy balance is more complicated than that for the gas-phase reactions of monomeric HgX, but reasonable agreement with experimental free energies can still be obtained. At present, energetics can be more easily and accurately assessed when using finite molecular cluster models than when using infinite periodic crystal models. Calculated differences in solubility and reactivity of HgO and HgS solids are in at least qualitative agreement with experiment.

What implications do these results have for Hg speciation in the Arctic troposphere and in the snowpack? Certainly the total concentrations of Hg species in the Arctic are small. A recent estimate[41] for the concentration of RGM is 300 pg/m^3, roughly equal to 1×10^{-15} M. However, our calculated reaction free energy for the formation of the chain triplet state of Hg_2O_2 from two molecules of singlet HgO is about −63 kcal/mol (from data in Tables 1, 3 and 5), corresponding to an equilibrium constant at 25 °C of about 10^{+46}, so that even at such low concentrations, most of the monomer would be converted to the dimer (if equilibrium is achieved). More probably, any monomeric HgO that forms will react very quickly with moisture in the air or with ice droplets to produce $Hg(OH)_2$.

Acknowledgment. This work was supported by NSF grant EAR-0001031 and DOE grant DE-FG02-94ER14467. Some of the COSMO hydration energy calculations were performed by using GAUSSIAN98 on the Carnegie Alpha Cluster, which is supported in part by NSF MRI grant AST-9976645.

References and Notes

(1) Schroeder, W. H.; Anlauf, K. G.; Barrie, L. A.; Lu, J. Y.; Steffen, A.; Schneeberger, D. R.; Berg, T. *Nature* **1998**, *394*, 331−332.

(2) Lu, J. Y.; Schroeder, W. H.; Barrie, L. A.; Steffen, A.; Welch, H. E.; Martin, K.; Lockhart, L.; Hunt, R. V.; Boila, G.; Richter, A. *Geophys. Res. Lett*. **2001**, *28*, 3219−3222.

(3) Steffen, A.; Schroeder, W.; Bottenheim, J.; Narayan, J.; Fuentes, J. D. *Atmos. Environ*. **2002**, *36*, 2653−2661.

(4) Lindberg, S.; Brooks, S.; Lin, C.-J.; Scott, K.; Landis, M. S.; Stevens, R. K.; Goodsite, M.; Richter, A. *Environ. Sci. Technol*. **2002**, *36*, 1245−1256.

(5) Barrie, L.; Platt, U. *Tellus, Ser. B* **1997**, *49*, 450−454.

(6) Schroeder, W. H.; Yarwood, G.; Niki, H. *Water, Air, Soil, Pollut.* **1991** *56*, 653−666.

(7) Pleijel, K.; Munthe, J. *Atmos. Environ*. **1995**, *29*, 1441−1457.

(8) Lin, C.-J.; Pehkonen, S. O. *Atmos. Environ*. **1999**, *33*, 2067−2079.

(9) Hall, B. *Water, Air, Soil, Pollut.* **1995**, *80*, 301−315.

(10) Sommar, J.; Gardfelt, K.; Stromberg, D.; Feng, X. *Atmos. Environ*. **2001**, *35*, 3049−3054.

(11) Ariya, P. A.; Khalizov, A.; Gidas, A. *J. Phys. Chem. A* 2002, 106, 7310−7320.

(12) (a) Grade, M.; Hirschwald, W. *Z. Anorg. Allg. Chem*. **1980**, *460*, 106−114. (b) Butler, R.; Katz, S.; Snelson, A.; Stephens, J. B. *J. Phys. Chem*. **1979** *83*, 2578−2580. (c) Grade, M.; Hirschwald, H. *Ber. Bunsen-Ges. Phys. Chem*. **1982**, *86*, 899−907.

(13) (a) Stromberg, D.; Gropen, O.; Wahlgren, U. *Chem. Phys*. **1989**, *133*, 207−219. (b) Stromberg, D.; Stromberg, A.; Wahlgren, U. *Water, Air, Soil, Pollut*. **1991**, *56*, 681−695. (c) Stromberg, D. Some Mercury Compounds Studied by Relativistic Quantum Chemical Methods, Ph.D. Thesis, Goteborg University and Chalmers University of Technology, 1990.

(14) Kaupp, M.; Dolg, M.; Stoff, H.; v. Schnering, H. J. *Inorg. Chem*. **1994**, *33*, 2122−2131.

(15) Shepler, B. C.; Peterson, K. A. *J. Phys. Chem. A* **2003**, *107*, 1783−1787.

(16) Tossell, J. A. *J. Phys. Chem. A* 2003, 107, 7804−7808.

(17) Filatov, M.; Cremer, D. *Chem. Phys. Chem*. 2004, 5, 1547−1557.

(18) (a) Tossell, J. A. *Am. Mineral*. **1999**, *84*, 877−883. (b) Tossell, J. A. *J. Phys. Chem. A* **1998**, *102*, 3587−3591. (c) Tossell, J. A. *J. Phys. Chem. A* 2000, 105, 935−941.

(19) *Introduction to Computational Chemistry*; Jensen, F., Ed.; Wiley: New York, 1999.

(20) Foresman, J. B.; Head-Gordon, M.; Pople, J. A.; Frisch, M. J. *J. Phys. Chem*. **1992**, *96*, 135−149.

(21) Pople, J. A.; Head-Gordon, M.; Raghavachari, K. *J. Chem. Phys*. **1987**, *87*, 5968−5975.

(22) Scuseria, G. E.; Janssen, C. L.; and Schaefer, H. F., III. *J. Chem. Phys*. **1988**, *89*, 7382−7387.

(23) Stevens W. J.; Krauss M.; Basch H.; Jansen P. G. *Can. J. Chem*. 1992, 70, 612−630.

(24) Truong, T. N.; Stefanovich, E. V. *Chem. Phys. Lett*. **1995**, *240*, 253−260.

(25) Schmidt M. W.; Baldridge, K. K.; Boatz, J. A.; Elbert, S. T.; Gordon, M. S.; Jensen, J. H.; Koseki, S.; Matsunaga, N.; Nguyen, K. A.; Su, S.; Windus,. T. L.; Dupuis, M.; Montgomery, J. A., Jr. *J. Comput. Chem*. **1993**, *14*, 1347−1363.

(26) (a) Frisch, M. J.; Trucks, G. W.; Schlegel, H. B.; Scuseria, G. E.; Robb, M. A.; Cheeseman, J. R.; Zakrzewski, V. G.; Montgomery, J. A., Jr.; Stratmann, R. E.; Burant, J. C.; Dapprich, S.; Millam, J. M.; Daniels, A. D.; Kudin, K. N.; Strain, M. C.; Farkas, O.; Tomasi, J.; Barone, V.; Cossi, M.; Cammi, R.; Mennucci, B.; Pomelli, C.; Adamo, C.; Clifford, S.; Ochterski, J.; Petersson, G. A.; Ayala, P. Y.; Cui, Q.; Morokuma, K.; Malick, D. K.; Rabuck, A. D.; Raghavachari, K.; Foresman, J. B.; Cioslowski, J.; Ortiz, J. V.; Stefanov, B. B.; Liu, G.; Liashenko, A.; Piskorz, P.; Komaromi, I.; Gomperts, R.; Martin, R. L.; Fox, D. J.; Keith, T.; Al-Laham, M. A.; Peng, C. Y.; Nanayakkara, A.; Gonzalez, C.; Challacombe, M.; Gill, P. M. W.; Johnson, B. G.; Chen, W.; Wong, M. W.; Andres, J. L.; Head-Gordon, M.; Replogle, E. S.; Pople, J. A. *Gaussian 98*, revision A.9.3; Gaussian, Inc.: Pittsburgh, PA, 1998. (b) Frisch, M. J.; Trucks, G. W.; Schlegel, H. B.; Scuseria, G. E.; Robb, M. A.; Cheeseman, J. R.; Montgomery, J. A., Jr.; Vreven, T.; Kudin, K. N.; Burant, J. C.; Millam, J. M.; Iyengar, S. S.; Tomasi, J.; Barone, V.; Mennucci, B.; Cossi, M.; Scalmani, G.; Rega, N.; Petersson, G. A.; Nakatsuji, H.; Hada, M.; Ehara, M.; Toyota, K.; Fukuda, R.; Hasegawa, J.; Ishida, M.; Nakajima, T.; Honda, Y.; Kitao, O.; Nakai, H.; Klene, M.; Li, X.; Knox, J. E.; Hratchian, H. P.; Cross, J. B.; Bakken, V.; Adamo, C.; Jaramillo, J.; Gomperts, R.; Stratmann, R. E.; Yazyev, O.; Austin, A. J.; Cammi, R.; Pomelli, C.; Ochterski, J. W.; Ayala, P. Y.; Morokuma, K.; Voth, G. A.; Salvador, P.; Dannenberg, J. J.; Zakrzewski, V. G.; Dapprich, S.; Daniels, A. D.; Strain, M. C.; Farkas, O.; Malick, D. K.; Rabuck, A. D.; Raghavachari, K.; Foresman, J. B.; Ortiz, J. V.; Cui, Q.; Baboul, A. G.; Clifford, S.; Cioslowski, J.; Stefanov, B. B.; Liu, G.; Liashenko, A.; Piskorz, P.; Komaromi, I.; Martin, R. L.; Fox, D. J.; Keith, T.; Al-Laham, M. A.; Peng, C. Y.; Nanayakkara, A.; Challacombe, M.; Gill, P. M. W.; Johnson, B.; Chen, W.; Wong, M. W.; Gonzalez, C.; Pople, J. A. *Gaussian 03*, revision B.03; Gaussian, Inc.: Wallingford, CT, 2004.

(27) Frisch, A. E.; Dennington, R. D.; Keith, T. A.; Nielsen, A. B.; Holder, A. J.; *GaussView*, revision 3.0, Gaussian, Inc., Pittsburgh, PA, 2003

(28) (a) Becke, A. *Phys. Rev. A* **1988**, *38*, 3098−3100. (b) Lee, C.; Yang, W.; Parr, R. G. *Phys. Rev. B* **1988**, *37*, 785−789. (c) Perdew, J. P.; Burke, K.; Ernzerrhof, M. *Phys. Rev. Lett.* **1996**, *77*, 3865−3868.

(29) (a) Charnock, J. M.; Moyes, L. N.; Pattrick, R. A. D.; Mosselmanjs, J. F.; Vaughan, D. J.; Livens, F. R. *Am. Mineral.* **2003**, *88*, 1197−1203. (b) Lennie, A. R.; Charnock, J. M.; Pattrick, R. A. D. *Chem. Geol*. **2003**, *199*, 199−207.

(30) Aurivillius, K. *Acta Crystallogr*. **1956**, *9*, 685−686.

(31) Auvreay, P.; Genet, F. *Bull. Soc. Fr. Mineral. Cristallogr*. **1973**, *96*, 218.

(32) Byrd, E. F.; Scuseria, G. E.; Chabalowski, C. F. *J. Phys. Chem. B* **2004**, *108*, 13100−13106.

(33) Ruiz, E.; Payne, M. C. *Chem.—Eur. J.* **1998**, *4*, 2485−2492.

(34) (a)Pal, B.; Ariya, O. A. *Phys. Chem. Chem. Phys*. **2004**, *6*, 572−579. (b) Raofie, F.; Ariya, P. A. *Environ. Sci. Technol*. **2004**, *38*, 4319−4326.

(35) Calvert, J. G.; Lindberg, S. E. *Atmos. Environ*. **2005**, *39*, 3355−3367.

(36) Benjelloun, A.; Daoudi, A.; Chermette, H. *J. Chem. Phys*. **2005**, *122*, 154304.

(37) Wang, X.; Andrews, L. *Inorg. Chem*. **2005**, *44*, 108−113.

(38) Benoit, J.; Gilmour, C.; Mason, R.; Heyes, A. *Environ. Sci. Technol*. **1999**, *33*, 951−957.

(39) Frost, R. L.; Martens, W. N.; Kloprogge, J. T. *Neues. Jahrb. Mineral., Monatsh.* **2002**, *10*, 469−480.

(40) Goodsite, M. E.; Plane, J. M. C.; Skov, H. *Environ. Sci. Technol*. **2004**, *38*, 1772−1776.

(41) Temme, C.; Einax, J. W.; Ebinghaus, R.; Schroeder, W. H. *Environ. Sci. Technol*. **2003**, *37*, 22−31.